Palaeogeography, Palaeoclimatology, Palaeoecology 600 (2022) 111062

Contents lists available at ScienceDirect

Palaeogeography, Palaeoclimatology, Palaeoecology

journal homepage: www.elsevier.com/locate/palaeo

Controls on the altitude of Scandinavian cirques: What do they tell us about palaeoclimate?

RachelP. Oien [a,*], Iestyn D. Barr [b], Matteo Spagnolo [a], Robert G. Bingham [c], Brice R. Rea [a], John Jansen [d]

[a] University of Aberdeen, School of Geosciences, Department of Geography & Environment, St. Mary's Building, Elphinstone Road, Aberdeen AB24 3TU, United Kingdom
[b] Manchester Metropolitan University, Department of Natural Sciences, Manchester M1 5GD, United Kingdom
[c] University of Edinburgh, School of GeoSciences, Drummond Street, Edinburgh EH8 9XP, United Kingdom
[d] GFU Institute of Geophysics, Czech Academy of Sciences, Prague, Czechia

ARTICLE INFO

Editor: P. Hesse.

Keywords:
ELA
Cirques
Palaeoclimate
Climate
Glacier

ABSTRACT

Cirques are glacially eroded, bowl-shaped depressions, characterised by steep headwalls and flat or over-deepened floors. Given their association with past glaciers, cirques are sometimes used as proxies for palaeoclimate. However, cirques are shaped over multiple glacial cycles, and their usefulness as palaeoclimate indicators therefore remains open to question. In this paper, we map 3984 glacier-free cirques across the Scandinavian Peninsula and analyse variations in cirque floor altitude (CFA). We explore the relationships between CFAs and cirque aspect, latitude, longitude, and distance to the coast. We test the validity of using CFAs as indicators of palaeoclimate through comparison with the equilibrium-line altitudes (ELAs) of 513 modern cirque glaciers. Results indicate that both CFAs and modern cirque-glacier ELAs decrease with latitude and vary with aspect, being generally lowest on east-facing slopes. However, the clearest and strongest trend in both CFAs and modern cirque glacier ELAs is an increase in elevation with distance from the modern coast (i.e., distance 'inland'). This likely indicates that similar climatic gradients, particularly an inland reduction in precipitation, acted to regulate former sites of glacier initiation (reflected by CFAs) and modern glacier ELAs. This would imply that CFAs are a useful proxy for palaeoclimate. However, we note that both CFAs and modern ELAs reflect the general topography of this region (with increasing elevations moving inland), and the glacial history of the area (indirectly linked to palaeoclimate) may have played a role in regulating where cirques have formed. For these reasons, we suggest that palaeoclimatic interpretations derived from CFAs should be treated with caution.

1. Introduction

The equilibrium-line altitude (ELA) is the elevation on a glacier surface where net annual accumulation and ablation are equal. Therefore, the ELA is largely determined by regional climate (the dominant control on accumulation and ablation) (Nesje, 1992; Ohmura et al., 1992; Ipsen et al., 2018; Ohmura and Boettcher, 2018), though other local topoclimatic factors (e.g. topographic shading, snow and ice redistribution and aspect) also contribute (Olyphant, 1977; Morris, 1981; Torsnes et al., 1993; Coleman et al., 2009; Hughes, 2010; Křížek and Mida, 2013). Given this association, glacier ELAs are often used to infer spatial and temporal variations in climate and palaeoclimate (e.g. Sutherland, 1984; Caseldine and Stotter, 1993; Torsnes et al., 1993; Oien et al., 2020; Rea et al., 2020). Therefore, palaeo-ELAs are important as palaeoclimatic indicators because they are the result of changed precipitation and temperature, which control glacial surface mass balance over time and cirques are one way of obtaining palaeo-ELAs (e.g. Torsnes et al., 1993; Bacon et al., 2010; Kern and László, 2010; Barr and Spagnolo, 2015a; Barr and Spagnolo, 2015b; Barr et al., 2017; Pearce et al., 2017; Ipsen et al., 2018; Wallick and Principato, 2020).

The most robust way to estimate palaeo-ELAs is to generate 3D reconstructions of former glaciers. However, a number of simpler methods are also used, particularly when considering ELAs across large and/or remote areas. One of the simplest ways is to map and measure cirque floor altitudes (CFAs) (e.g. Torsnes et al., 1993; Kern and László, 2010; Barr and Spagnolo, 2015a; Barr and Spagnolo, 2015b; Barr et al., 2017;

* Corresponding author.
E-mail addresses: rachel.oien1@abdn.ac.uk (RachelP. Oien), I.Barr@mmu.ac.uk (I.D. Barr), m.spagnolo@abdn.ac.uk (M. Spagnolo), r.bingham@ed.ac.uk (R.G. Bingham), b.rea@abdn.ac.uk (B.R. Rea), jdj@ig.cas.cz (J. Jansen).

https://doi.org/10.1016/j.palaeo.2022.111062
Received 7 June 2021; Received in revised form 6 May 2022; Accepted 17 May 2022
Available online 21 May 2022

Pearce et al., 2017; Ipsen et al., 2018; Wallick and Principato, 2020). The premise behind this approach is that cirques (bowl-shaped depressions, characterised by steep headwalls and flat or overdeepened floors sometimes occupied by small lakes; Evans and Cox, 1974; Vilborg, 1977; Fredin, 2002) are formed where glaciers develop and erode their underlying bedrock. When these glaciers are relatively small and largely confined to the cirque (e.g., at the onset and termination of glacial cycles), the CFA (i.e., the lowest point within a cirque) roughly approximates the glacier's ELA. Though this approach only provides an approximation of the ELAs of former cirque glaciers, it has been widely used to investigate regional patterns in palaeo-ELAs, and sometimes to make associated inferences about palaeoclimate (e.g. Evans, 1999; Benn and Lehmkuhl, 2000; Barr and Spagnolo, 2015b). Despite this widespread use, there are several caveats associated with using CFAs as indicators of former cirque glacier ELAs. In particular, since cirque glaciers form at different times in different places, regional trends in CFA are unlikely to reflect palaeo-ELA trends at any single point in time. This raises questions about the usefulness of CFAs as proxies for palaeoclimate.

In this study, we map the distribution of glacier-free cirques in the Scandinavian Mountains and analyse variations in the associated CFAs. We compare these patterns with the ELAs of modern cirque glaciers in the region (Oien et al., 2020). The aim is to establish how palaeoclimatic information can most efficiently be extracted from cirque floor elevation distributions, despite their potentially time-transgressive origins, evolution and occupation (Rudberg, 1994; Evans, 1999; Barr and Spagnolo, 2013). The Scandinavian Mountains are well suited to this study, as they lie on a passive margin, have a comparatively well-constrained glacial history, and both cirques and extant cirque glaciers are widespread.

2. Study Area

2.1. Geology and Geography

The study area (Fig. 1) extends ~2000 km N-S along the Scandinavian Mountains, and up to 400 km W-E from the Norwegian Sea inland into Sweden. Topographic elevations typically increase inland, extending up to ~1500 m in the north and ~ 2400 m in the south. The geology is mostly a result of the Caledonian orogeny, from 400 to 700 Ma (Holtedahl, 1920; Stephens, 1988; Lidmar-Bergström et al., 2000), when collisions between orogenic belts and exotic terranes created a series of Precambrian and Palaeozoic crystalline metamorphic rocks (Pawlewicz et al., 2002; Etzelmüller et al., 2007). The closure of the Iapetus Ocean and collision with Laurentia caused crustal thickening, generating a stable crust that makes up the Fennoscandian Shield (Stephens, 1988). The majority of cirques in the south are located within areas classified as upland mountains with moderate slopes and alpine relief (Etzelmüller et al., 2007). This region is known for extensive plateaux steeply cut by glacial valleys (Etzelmüller et al., 2007). More recently, glacial isostatic adjustment due to the demise of the Fennoscandian ice sheet has resulted in an uplift of up to ~1 to 15 mm yr^{-1} across the Scandinavian Peninsula (Lambeck et al., 1998a; Lambeck et al., 1998b; Steffen and

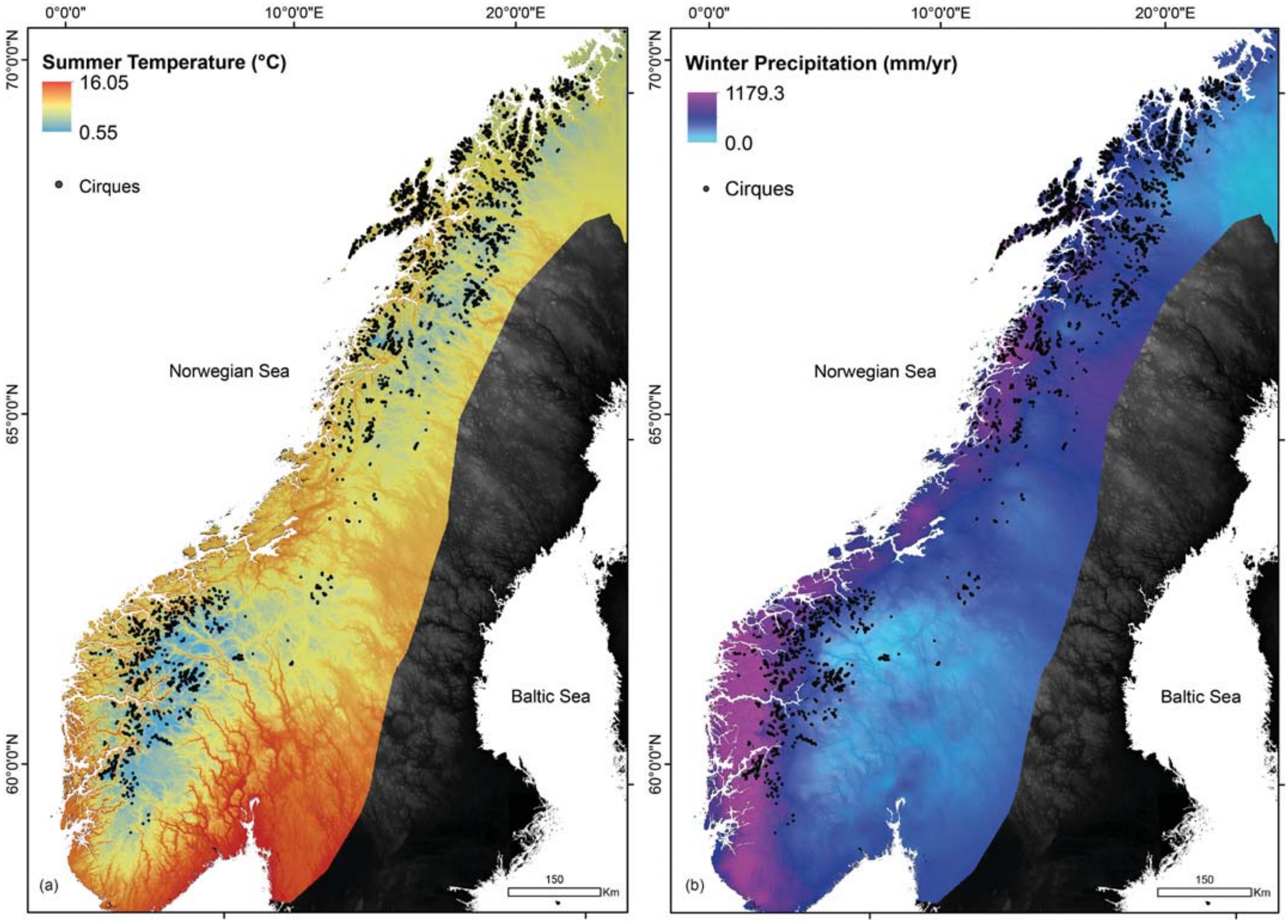

Fig. 1. (a) Mean summer air temperature (JJA) and (b) total winter precipitation (DJF) patterns for present-day Scandinavia (NVE, 2017). Winter precipitation and summer temperatures are averaged over 30 years from 1971 to 2000 (NVE, 2017).

Kaufmann, 2005; Argus and Peltier, 2010).

2.2. Glaciation

Extensive glaciers and ice sheets have repeatedly occupied and shaped the Scandinavian landscape over multiple Quaternary (and pre-Quaternary) glacial cycles (e.g. Mangerud, 2008; Mangerud et al., 2011; Fredin, 2002; Olsen et al., 2013a; Olsen et al., 2013b; Hughes et al., 2016; Stroeven et al., 2016). These glaciations have generated a wide range of erosional and depositional features, resulting in a dramatic landscape of elongated overdeepened basins (often occupied by lakes), fjords, glacial valleys, and cirques. At present, thousands of glaciers occupy the Scandinavian Mountains, ranging in size from small cirque glaciers to extensive ice caps (Nesje, 2009; NVE, 2017).

2.3. Climate

Climatic patterns across the Scandinavian Peninsula are heavily influenced by the North Atlantic Oscillation (NAO) and Arctic Oscillation (AO) (Nesje et al., 2008). These systems regulate pressure gradients, which control temperature, precipitation, and storms. The interplay of these pressure systems sometimes results in comparatively warm (between 0 and 2 °C) wet (up to 2000 mm/year in the southern coastal region) winters, or cold (between 0 and − 16 °C, particularly in the northern region) dry winters (Norwegian Meteorological Institute, 2021). In the southern Scandinavian Mountains, precipitation is also regulated by the Jet Stream, with a dominant wind direction from the S/SW, and can reach 6000 mm/year in coastal areas but decreases dramatically inland to 500–750 mm/year (Torsnes et al., 1993; Nesje et al., 2008; Nesje, 2009; Winsvold et al., 2014; Norwegian Meteorological Institute, 2021). Winter precipitation (Fig. 1b) and summer temperatures (Fig. 1a) are the main climatic controls on modern-glacier surface mass balance (Ohmura et al., 1992; NVE, 2017; Ohmura and Boettcher, 2018; Oien et al., 2020).

3. Methods

We mapped glacier-free cirques using a 10 × 10 m digital terrain model (DTM) with a vertical accuracy of ±1–6 m, overlain with 10 m contours from the Norwegian mapping authority (Kartverket; Hoydedata.no; Norwegian Mapping Authority, 2016) (Fig. 2). Most of the mapped cirques coincide with cirque locations identified by Rudberg (1994) and the definition of a cirque by Evans and Cox (1974) and Vilborg (1984). Once mapped, we divided cirques by latitude into southern <64°N and northern >64°N sub-populations ('macro-regions'), following Oien et al. (2020). The division is roughly based on climate, with the northern macro-region defined as 'polar/subpolar' due to its proximity to the polar front while the southern macro-region is 'temperate' due to the influence of the North Atlantic Current (Tveito et al., 2000; Oien et al., 2020).

Each cirque was mapped as a polygon (Fig. 2): we extracted the CFA as the single lowest elevation DTM grid cell contained within the polygon (Fig. 3a). To assess possible controls on CFA, several other attributes were derived: cirque aspect was calculated using the GIS tool ACME (Spagnolo et al., 2017) (i.e. aspect is defined as the mean azimuth (0–360°) determined from every pixel converted to radians and averaged within the cirque) (Evans, 1977; Evans, 2006b; Barr and Spagnolo, 2015a); cirque latitude and longitude were recorded using the centroid of each feature; and cirque distance from the modern coast, excluding fjords (Norwegian Sea, Fig. 3) was calculated in ArcGIS (following Oien et al., 2020). In addition to mapping cirques, the ELAs of 513 modern cirque glaciers (Fig. 3b) in the region were analysed, based on the dataset from Oien et al. (2020).

4. Results

4.1. Cirque-floor altitudes (CFAs)

A total of 3984 glacier-free cirques were mapped throughout the

Fig. 2. An example of two of the mapped glacier-free cirque outlines (in pink) overlayed in Google Earth, located at 62°28′43.97"N 7°57′41.59″E. (For interpretation of the references to colour in this figure legend, the reader is referred to the web version of this article.)

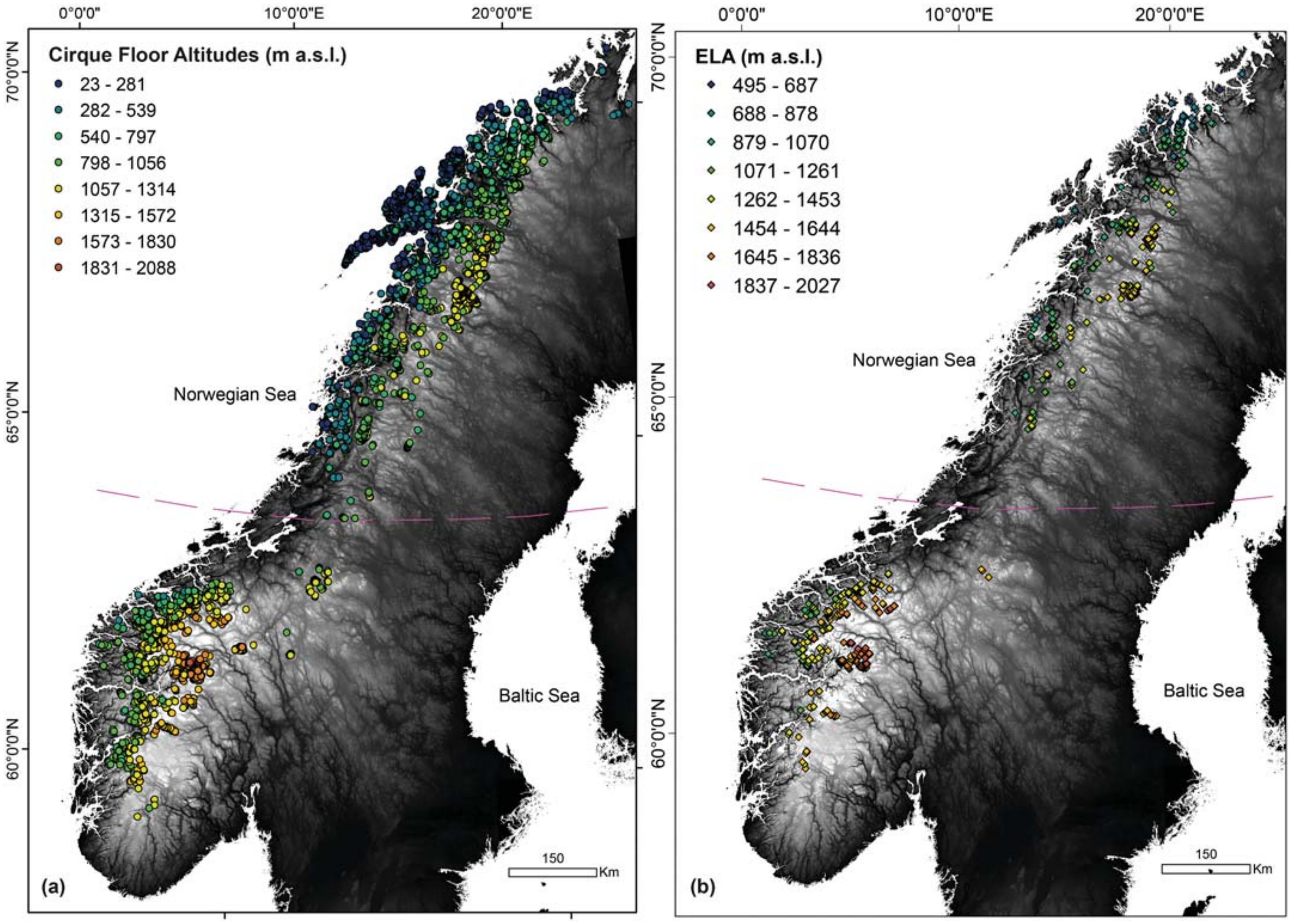

Fig. 3. (a) Cirque floor altitudes and (b) modern-glacier ELAs. The dashed line separates regions termed in the text as the northern and southern regions.

Scandinavian Mountains: 2947 in the northern region, and 1037 in the southern region (Fig. 3). For the population as a whole, CFAs range from 23 m to 2088 m (Table 1). In the northern region, the mean CFA (591 m) is notably lower than in the southern region (1195 m). Cirques in the northern region are also typically closer to the modern coastline (mean distance = 40.8 km) than those in the south (mean distance = 104.7 km) (Table 2).

4.2. CFA variations with latitude and longitude

For the population as a whole, CFAs show a statistically significant, $p < 0.01$, decline to the north and east (Fig. 4), although the linear regression between CFA and latitude is stronger ($R^2 = 0.441$) than between CFA and longitude ($R^2 = 0.212$). Despite these general trends, considerable variability is present between each (southern and northern) region. For example, in the northern region, CFAs decline with

Table 1
Cirque floor altitudes (cirques) and ELAs (modern mountain glaciers) across the Scandinavian Peninsula, subdivided by region.

	Total population (cirques)	Northern region (cirques)	Southern region (cirques)	Total population (glaciers)	Northern region (glaciers)	Southern region (glaciers)
Number	3984	2947	1037	513	258	255
Min (m a.s.l.)	23	23	287	495	495	788
Max (m a.s.l.)	2088	1610	2088	2027	1639	2027
Mean (m a.s.l.)	745	591	1195	1339	1151	1528
Median (m a.s.l.)	721	541	1166	1368	1158	1519
Std. dev (m a.s.l.)	422	333	311	303	245	229

Table 2
Summary statistics for the CFAs/ELAs and distance to the coast within the northern and southern regions for cirques and modern glaciers. All characteristics were extracted using ACME (Spagnolo et al., 2017).

	Northern cirques (n = 2947)			Northern modern glaciers (n = 258)		
	Mean	Median	Std. deviation	Mean	Median	Std. deviation
CFA/ELA (m a.s.l.)	591	541	333	1151	1158	245
Distance to the coast (km)	40.83	27.01	36.3	67.73	64.97	33.16

	Southern cirques (n = 1037)			Southern modern glaciers (n = 255)		
	Mean	Median	Std. deviation	Mean	Median	Std. deviation
CFA/ELA (m a.s.l.)	1195	1166	311	1528	1519	229
Distance to the coast (km)	104.67	96.98	43.32	108.18	97.65	42.09

latitude (Fig. 5; $R^2 = 0.113$, panel a), but more weakly than for the entire cirque population. In the southern region, CFAs rise then fall with latitude (Fig. 6; $R^2 = 0.114$, panel a). Overall, it appears that the population-wide latitudinal trend in CFA is partly a reflection of differences between the northern and southern regions (Fig. 4a). In both the northern and southern regions, CFAs show an eastward rise then fall with longitude (Fig. 5b, Fig. 6b). The ELAs of modern cirque glaciers in the region show broadly similar latitudinal and longitudinal trends to those highlighted for the CFA population (and sub-populations) but as expected, lie a few hundred metres above (Fig. 4a, b, 5a, b, 6a, b).

4.3. CFA variations with aspect

The mean vector aspect for the entire cirque population is 35.5°, which compares with 40.7° for modern cirque glaciers. However, these values show some regional variation. In the northern region, the cirque and modern cirque glacier vector means are 36.5° and 42.8°, respectively. In the southern region, these values are 33.2° and 38.4°, respectively (Fig. 7). However, overlapping 95% confidence intervals suggest that inter-regional differences in mean aspect (Fig. 7) are unlikely to be statistically significant. CFAs and modern cirque glacier ELAs show some variability with aspect. For example, *E*-facing cirques typically have lower CFAs by ~150 m (median = 642 m) than those facing S/SW (median = 828 m) (Fig. 8), for the entire population. Fourier (harmonic) regression (Evans and Cox, 1974; Evans, 2006a) indicates that these relationships show no statistically significant overall trends, $p > 0.05$ (Table 3). Aspect vector strength for the entire cirque population is 29%, which compares to 69% for the modern cirque glaciers. This difference likely stems from the entire cirque population reflecting conditions during multiple periods of past glaciation, whereas the distribution and aspect of modern cirque glaciers reflects conditions during a single 'snapshot' of marginal glaciation (i.e., the present) when topoclimatic factors (e.g. shading) play a strong role in regulating glacier location. This is consistent with the 'law of decreasing glacial asymmetry with increasing glacier cover' (Evans, 1977).

4.4. CFA variations with distance to the coast

The attribute most strongly related to CFA is the distance to the

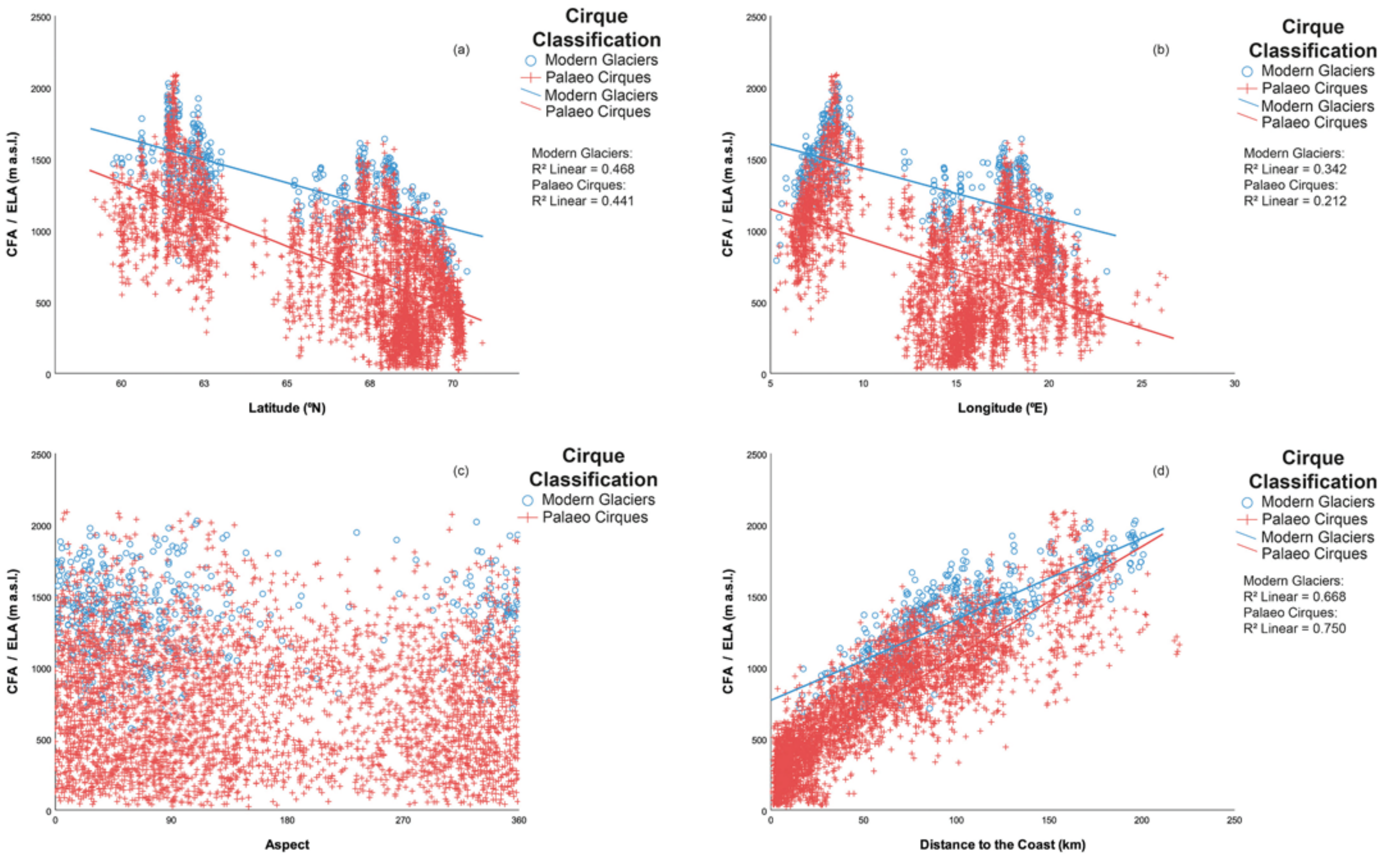

Fig. 4. Variations in cirque floor altitudes and glacier ELAs, with: (a) latitude; (b) longitude; (c) aspect; and (d) distance to the modern coastline.

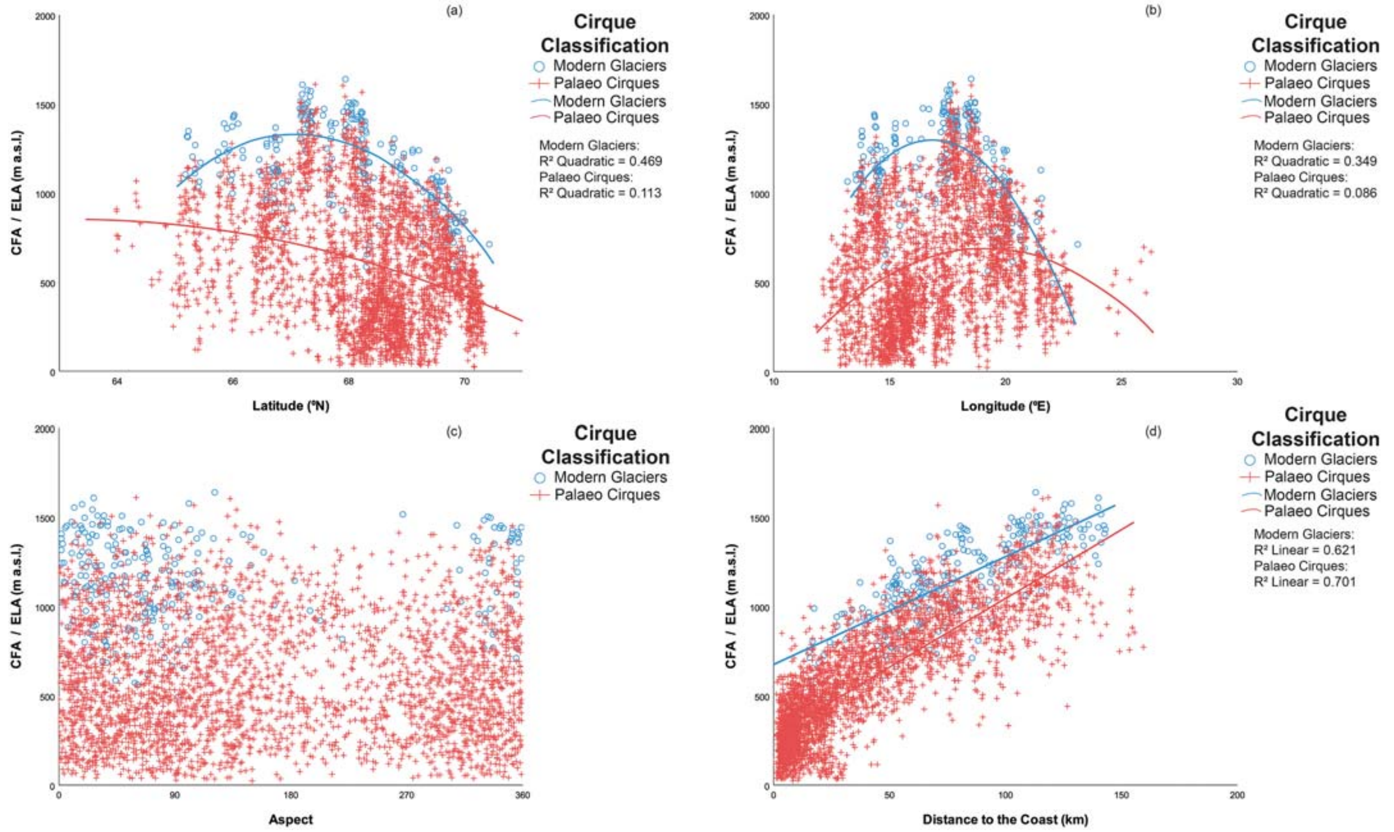

Fig. 5. Variations in cirque floor altitudes and glacier ELAs in the northern region with: (a) latitude; (b) longitude; (c) aspect; (d) distance to the modern coastline.

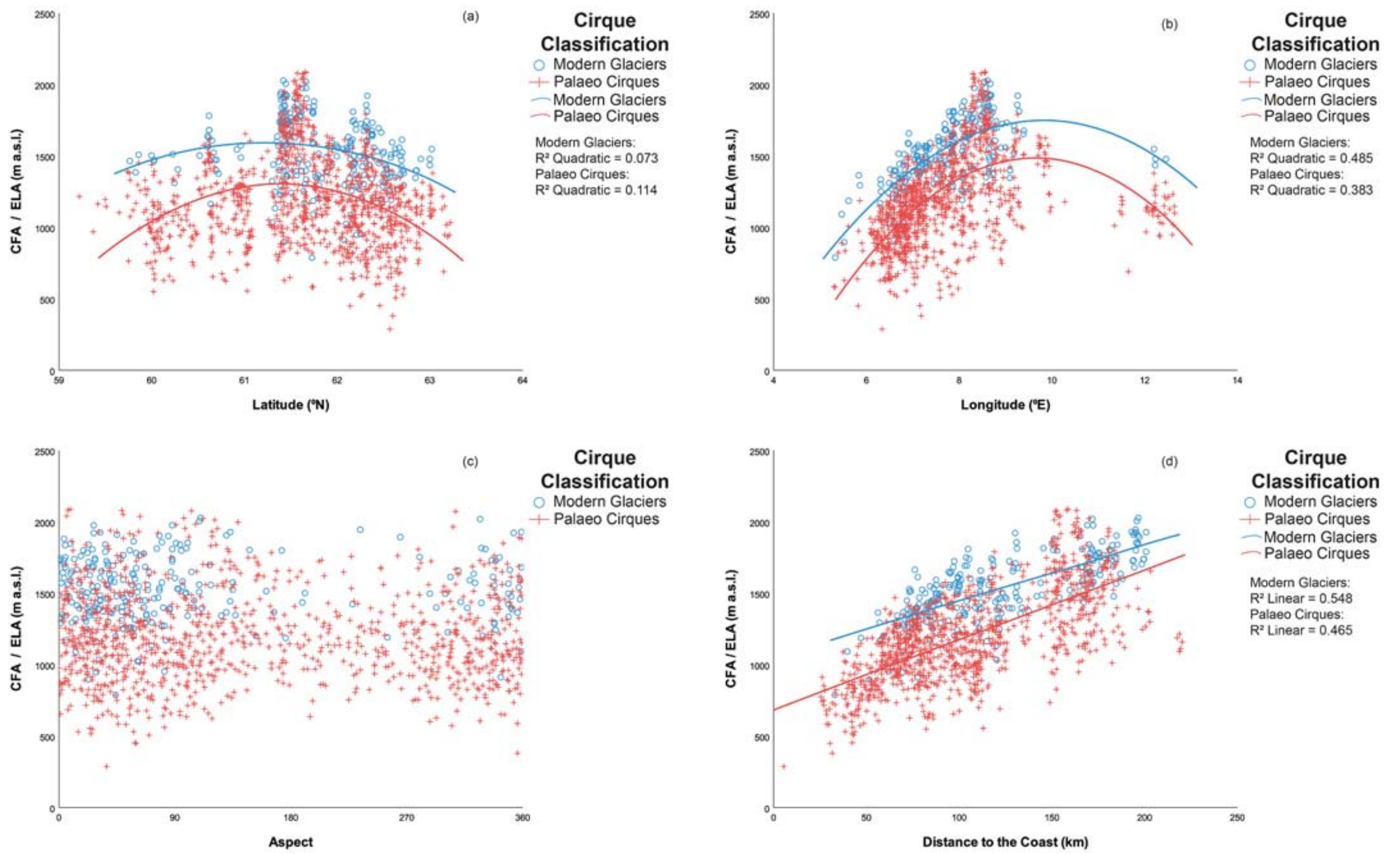

Fig. 6. Variations in cirque floor altitudes and glacier ELAs in the southern region with: (a) latitude; (b) longitude; (c) aspect; (d) distance to the modern coastline.

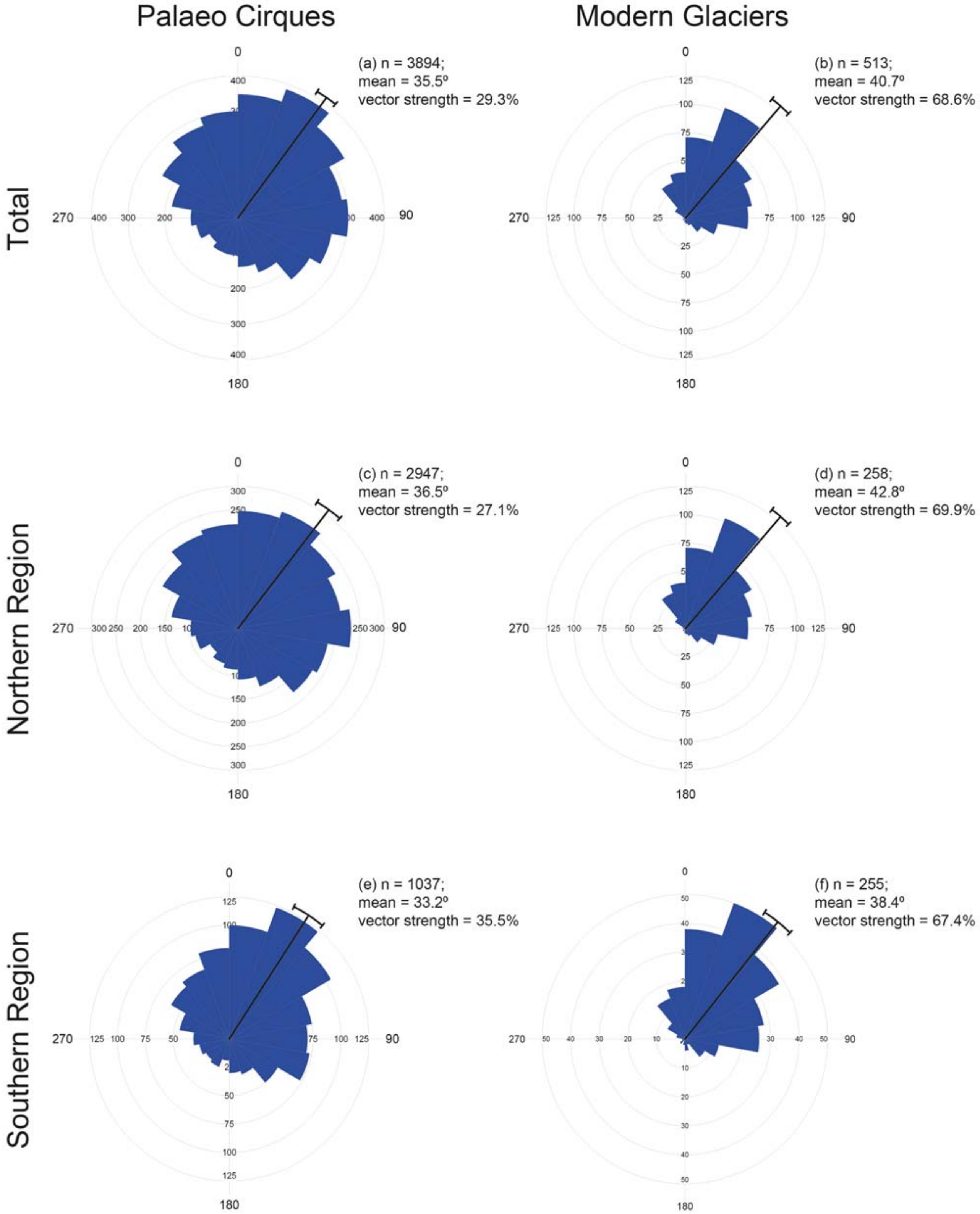

Fig. 7. Rose diagrams (linear scale of frequency with equal bin widths) of mean vector aspect frequency and vector strength. (a) Entire cirque population, (b) entire modern cirque glacier population, (c) cirques in the northern region, (d) modern cirque glaciers in the northern region, (e) cirques in the southern region, (f) modern cirque glaciers in the southern region. In each Rose diagram, the line represents the vector mean and the bar (on the end of each line) shows the 95% confidence interval. (For interpretation of the references to colour in this figure legend, the reader is referred to the web version of this article.)

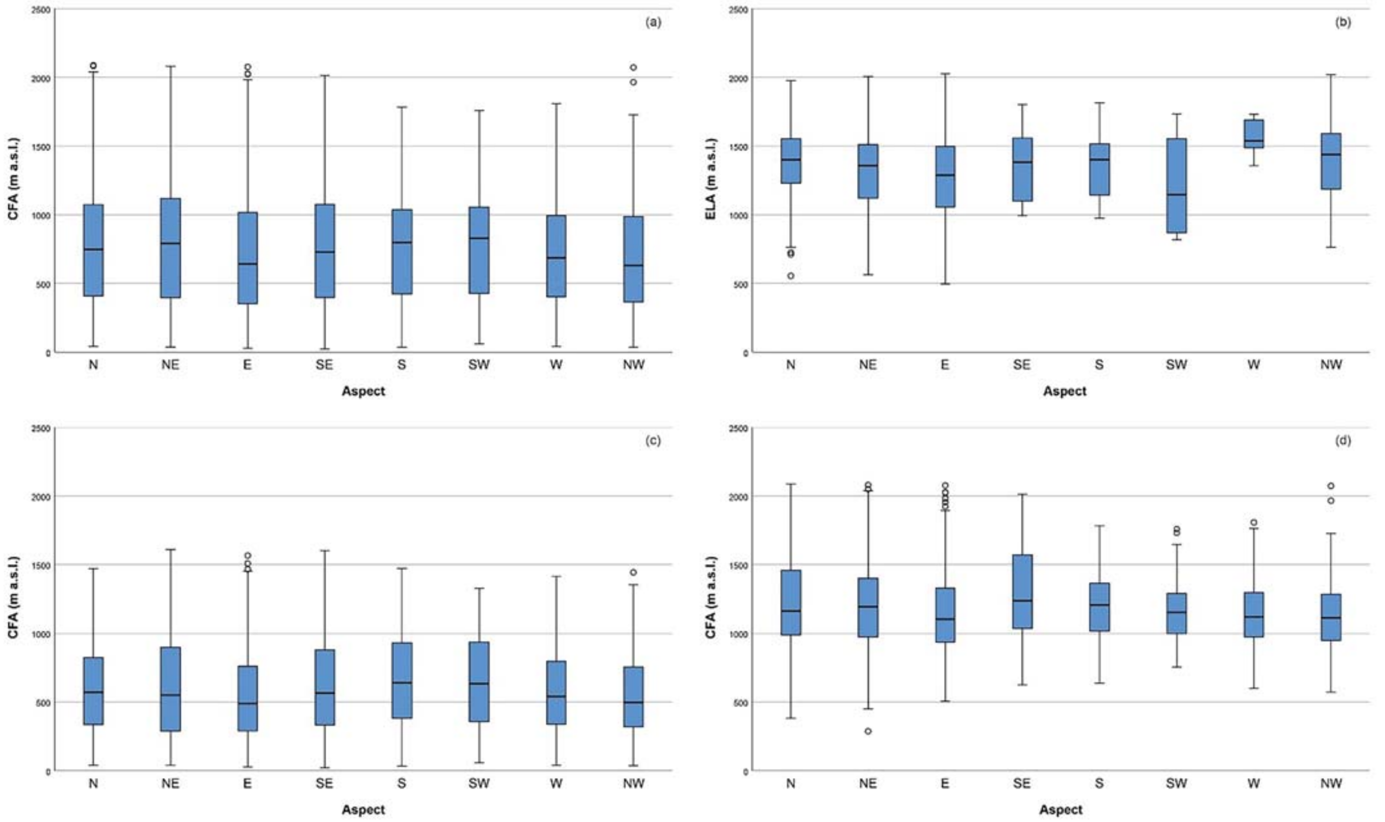

Fig. 8. Boxplots comparing the CFA or ELA with aspect for the (a) whole cirque dataset (b) modern cirque glaciers (c) northern cirque region (d) southern cirque region. The thick middle line indicates the median, the top and bottom of the box represent the 1st and 3rd quartiles and the edge of the whisker represent the range, maximum and minimum excluding outliers. Outliers (open circles) are defined as points which lie more than 1.5 box lengths beyond the interquartile range. The number of modern glaciers and cirques within each aspect group is shown in Table 4.

modern coastline, with the population as a whole (7.7 m/km; $R^2 = 0.750$; RMSE = 211; Fig. 4d) and northern (7.7 m/km; $R^2 = 0.701$; RMSE = 182; Fig. 5d) and southern (4.9 m/km; $R^2 = 0.465$; RMSE = 227; Fig. 6d) sub-regions showing a statistically significant increase inland, $p < 0.01$ (Table 3). This trend is also seen in modern cirque glacier ELAs as a whole (5.8 m/km; $R^2 = 0.668$; RMSE = 177; Fig. 4d) and within the northern (6.1 m/km; $R^2 = 0.621$; RMSE = 134; Fig. 5d) and southern (3.8 m/km; $R^2 = 0.548$; RMSE = 155; Fig. 6d) regions. For both CFAs and modern cirque glacier ELAs, the relationship with distance to the coastline is stronger in the northern region (where cirques and glaciers are also typically closer to the coast) than in the southern region. The inland increase in CFAs and modern cirque glacier ELAs follows the overall topographic gradient of the Scandinavian Mountains, with elevations increasing inland. These data illustrate that in each region, distance from the modern coastline is the individual variable that shows the strongest relationship with CFA (as indicated by R^2 and RMSE). In each region, multiple regression of CFA against latitude, longitude and distance from the modern coastline returns the highest R^2 and lowest RMSE. However, distance from the modern coastline dominates these relationships (i.e. it is consistently the variable with the strongest *t* value), and they only differ slightly from those based on CFA and distance from the coastline alone (Table 3).

5. Discussion

Cirque morphology, aspect, and elevation, including CFAs, are thought to represent a time-transgressive record of climatic and glaciological conditions during former periods when cirques were occupied periodically by erosive (warm-based) ice (Meierding, 1982; Barr and Spagnolo, 2013; Ipsen et al., 2018). These conditions occurred multiple times during the Quaternary (and pre-Quaternary) in Scandinavia, but usually towards the onset and termination of each glacial cycle. By contrast, modern cirque glacier ELAs only (or largely) reflect climatic conditions at a single period in time (i.e., the present), when glaciers are experiencing generalised retreat. Given this difference, here we discuss the factors that potentially control CFAs and modern cirque glacier ELAs and assess if, and how, these differ. From this, we consider what CFAs can tell us about palaeoclimate.

5.1. Factors controlling CFAs and modern cirque glacier ELAs

5.1.1. Climate

Across the study region, the northward decline in CFAs and modern cirque glacier ELAs (Fig. 4a), although to some degree a function of the two sub-regions, suggests that a latitudinal decline in air temperatures played a role in regulating the altitude at which former mountain glaciers were able to initiate (generating cirques) and regulates where cirque glaciers are currently able to exist (Renssen et al., 2001; Fredin, 2002; Ipsen et al., 2018). However, since this latitudinal decline in CFAs is far less apparent when sub-populations (i.e., northern and southern) are considered (Fig. 5a & 6a), it is likely that this control mostly operates over large spatial scales (Bakke et al., 2008). More locally, there is evidence that topographic sheltering and/or shading (as reflected by cirque and cirque glacier aspects) plays a role in regulating CFAs and modern ELAs, suggesting that glacier initiation and sustenance was/is promoted at lower altitudes on east-facing slopes (Fig. 8) (Olyphant, 1977; Hassinen, 1998).

Despite the evidence for air temperature and aspect-related controls, the strongest region-wide pattern in both CFAs and modern cirque glacier ELAs is an increase with distance inland, which corresponds to

Table 3
Regression of cirque floor altitude (CFA) against latitude (Lat), longitude (Lon), distance from the modern coastline (D), and aspect (α). Significant relationships (i.e., where $p < 0.01$*, $p < 0.05$**), other than those based on multiple regression, are shown in Figs. 3-5. For equations based on multiple regression, the coefficient and variable with the strongest *t* value are in **bold**.

Region	Variable	Equation	*p*-value	R^2	RMSE (m)
Total	Lat	CFA = −88.74Lat + 6659.64	<0.01*	0.441	315
	Lon	CFA = −41.63Lon + 1356.03	<0.01*	0.212	374
	Dist (D)	CFA = 7.70D + 305.86	<0.01*	0.750	211
	Aspect (α)	Not stat. Sig.	0.31	n/a	n/a
	Lat, lon, dist (D)	CFA = −85.40Lat + 35.78Lon + **5.49D** + 5598	<0.01*	0.778	199
Northern	Lat	CFA = −9.60Lat^2 + 1215.10Lat - 37,603	<0.01*	0.113	314
	Lon	CFA = −8.95Lon^2 + 342.36Lon - 2586	<0.01*	0.086	319
	Dist (D)	CFA = 7.69D + 277	<0.01*	0.701	182
	Aspect (α)	CFA = −23.90cosα −1.24sinα + 596.45	0.03**	n/a	n/a
	Lat, lon, dist (D)	CFA = −108.46Lat + 51.38Lon + **5.58D** + 6902	<0.01*	0.731	174
Southern	Lat	CFA = −135.14Lat^2 + 16589Lat - 507,781	<0.01*	0.114	293
	Lon	CFA = −53.38Lon^2 + 1030.40Lon – 3489	<0.01*	0.383	244
	Dist (D)	CFA = 4.90D + 682	<0.01*	0.465	227
	Aspect (α)	Not stat. Sig.	0.06	n/a	n/a
	Lat, lon, dist (D)	CFA = 121.92Lat – 65.04Lon + **6.54D** – 6505	<0.01*	0.503	219

Table 4
Number of modern glaciers and cirques within each aspect group. N, 337.5–22.5°; NE, 22.5–67.5°; E, 67.5–112.5°; SE, 112.5–157.5°; S, 157.5–202.5°; SW, 202.5–247.5°; W, 247.5–292.5°; NW, 292.5–337.5.

	N	NE	E	SE	S	SW	W	NW
Modern glaciers (total)	136	181	114	25	10	4	6	37
Modern glaciers (North)	67	88	64	13	4	2	1	19
Modern glaciers (South)	69	93	50	12	6	2	5	18
Cirques (total)	742	779	629	477	263	233	316	545
Cirques (North)	527	534	475	371	210	176	237	417
Cirques (South)	215	245	154	106	53	57	79	128

present-day prevailing wind direction (W/SW to E/NE). Similar inland trends are found in other regions and are thought primarily to reflect a limit to favourable glacial conditions, imposed by a gradual inland reduction in precipitation (Peterson and Robinson, 1969; Nesje et al., 2008; Principato and Lee, 2014; Barr and Spagnolo, 2015a; Barr et al., 2017; Ipsen et al., 2018; Wallick and Principato, 2020). In Scandinavia specifically, this logic implies that, exposure to moisture from the Norwegian Sea is a key factor controlling former sites of glacier initiation and modern glacier ELAs (Bakke et al., 2008; Nesje et al., 2008; Evans, 2011; Oien et al., 2020). Present-day precipitation shows a strong relationship with modern cirque glacier ELAs in Scandinavia (Winkler et al., 2009; Oien et al., 2020). Our CFA study suggests that palaeoprecipitation gradients similar to present-day might have existed during periods of the Quaternary (or earlier) when cirques formed and were subsequently re-occupied by cirque glaciers. This long-term stability of climatic gradients in the region has been suggested previously, as other palaeoclimatic proxies have shown, for example, that maritime wet conditions were recurrent throughout the Holocene in the coastal part of the southern region of Scandinavia (Seppä and Birks, 2001; Bjune et al., 2005; Bakke et al., 2008). Furthermore, palaeoclimate models, extending through the last glaciation maximum and Younger Dryas, show an overall pattern of precipitation decreasing inland (e.g. Renssen et al., 2001; Forsström, 2005; Rea et al., 2020).

For the region as a whole, and the two sub-regions, the inland increase in CFAs has a slightly steeper gradient than the increase in modern ELAs. Barr and Spagnolo (2015b) found a similar trend between CFAs and modern glacier ELAs in Kamchatka (Eastern Russia). They attributed this difference to the fact that CFAs reflect sites of former glacier initiation (largely controlled by snowfall), while modern glacier ELAs are also strongly regulated by the variety of topoclimatic factors which control ablation (i.e., the link to precipitation is weakened, and modern glaciers can survive even in regions with limited snowfall). This difference in the factors controlling CFAs and modern ELAs might also apply in Scandinavia. However, it is also possible that the steeper inland CFA gradient (when compared to modern glacier ELAs) in Scandinavia reflects the control of ice sheet growth on areas suitable for cirque formation (see Section 5.1.3).

5.1.2. *Topography*

Topographic availability exerts a control on where glaciers can develop, e.g. high-altitude glaciers can only form where high-altitude topography exists. Therefore, regional trends in CFAs and modern glacier ELAs likely partly reflect topographic (i.e. mountain elevation) gradients. Oien et al. (2020) considered the potential role of topography in controlling modern cirque glacier ELAs across Scandinavia and found that mean topography and modern ELAs increase inland with similar gradients. Results from the present study reveal that CFAs also increase inland, with very similar (but slightly steeper) gradients. Studies in other regions globally have contemplated the possible role that topographic gradients play in regulating CFAs (e.g., Peterson and Robinson, 1969; Hassinen, 1998; Dahl and Nesje, 1992; Anders et al., 2010; Mitchell and Humphries, 2014; Barr and Spagnolo, 2015b; Barr et al., 2017; Wallick and Principato, 2020). Though these studies acknowledge the role of topography, most conclude by suggesting that palaeoprecipitation gradients (as indicated by cirque distance from the coast) are likely the dominant control on CFAs. In Scandinavia specifically, Hassinen (1998), focusing on an area at the very north of our study, considered the inland increase in CFAs to reflect palaeoprecipitation gradients combined with topographic trends (i.e., mountain heights gradually increase to the east, but at a slower rate than CFAs). Similarly, Oien et al. (2020) concluded that inland precipitation reduction and topographic gradients likely act together to regulate modern cirque glacier ELAs in the Scandinavian Mountains. The results from the present study support the idea that, as with modern cirque glacier ELAs, trends in CFAs are, to some degree, dictated by topography. This is illustrated in Fig. 9, which suggests that neither ELA gradients nor topographic gradients alone can explain the inland cirque distribution observed in Scandinavia. The former fails to explain the absence of high-altitude cirques near the coast (Fig. 9a), and the latter fails to explain the absence of low-altitude cirques further inland (Fig. 9b). However, when both inland ELA gradients and topographic gradients are considered, observed CFA trends are understandable (Fig. 9c).

5.1.3. *Glacial history*

During glacial periods, large ice masses readily develop in the Scandinavian Mountains and coalesce to form an ice sheet (e.g. Mangerud, 2008; Mangerud et al., 2011; Fredin, 2002; Olsen et al., 2013a; Hughes et al., 2016). In Scandinavia, these large ice masses first occupy the highest mountains of the interior of the southern region, and gradually advance and coalesce to cover the entire peninsula (Fredin, 2002; Kleman et al., 2008; Mangerud et al., 2011; Olsen et al., 2013a; Olsen et al., 2013b). Once a landscape is submerged by ice, 'new' cirques cannot form and existing cirques experience minimal modification. Thus, in interior locations (i.e., far from the coast), the formation of

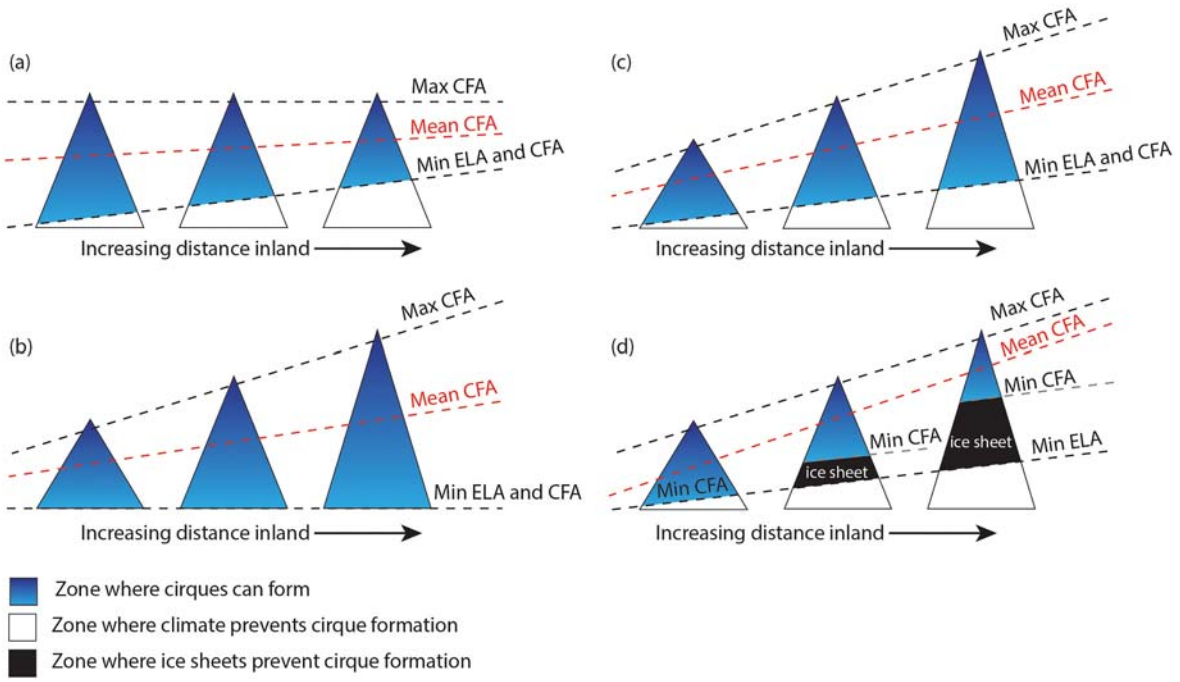

Fig. 9. Schematic illustration of potential drivers of the inland increase in minimum, mean and maximum CFAs observed in the present study. (a) Climatic gradient alone (as indicated by variability in climatic ELA), (b) topographic gradient alone, (c) climatic and topographic gradients, (d) climatic and topographic gradients, combined with spatial variability in glacial history, with the top of the black margin representing the minimum CFA (i.e., the formation of ice sheets at inland locations) and the bottom the minimum ELA. This illustration indicates that only scenarios (c) and (d) produce CFA distributions comparable to that seen in Fig. 4d, despite the complex history of uplift in the Scandinavian Mountains (Nielsen et al., 2009; Steer et al., 2012; Pedersen et al., 2021).

'new', and modification of existing, cirques likely stop comparatively early during the onset of glacial periods (when the local ELA is still relatively high), since the landscape quickly becomes entirely submerged by largely cold-based (i.e. non erosive) ice extending from local high-altitude regions of ice-sheet initiation. By contrast, in coastal locations the local ELA may drop close to sea level (as indicated by CFAs), before the landscape is submerged by an ice sheet (Rudberg, 1994; Dahl et al., 1997; Hassinen, 1998; Nesje, 2009).

This means that in Scandinavia low-altitude cirques can only develop in coastal locations, and not in interior regions. It is reasonable to assume that the lowest elevation cirques, particularly those along the modern-day coast in the northern region (Fig. 3a), would only be filled at times of extensive glaciation (Agrell, 1977; Olyphant, 1977; Dahl et al., 1997; Batchelor et al., 2019). This spatial difference in glacial history is likely to enhance the inland trend in CFAs (already dictated by climate and topography – see sections 5.1.1., and 5.1.2.) (Fig. 9d) and might help explain why inland gradients in CFAs are slightly steeper than modern ELA gradients.

5.1.4. Additional factors

In previous studies elsewhere, spatial variations in glacio-isostatic adjustment and former glacial erosion rates (linked to ice dynamics and subglacial geology) have been considered as possible explanations for region-wide trends in CFA (e.g., Bakke et al., 2005; Barr and Spagnolo, 2015b; Barr et al., 2017). However, in Scandinavia, there is little evidence to suggest that these factors control the trends in CFAs. For example, all the cirques analysed in this study are currently experiencing glacio-isostatic uplift (Rosentau et al., 2012), and those in interior regions are experiencing more rapid and greater uplift than in coastal locations (Rosentau et al., 2012). This means that cirques in interior locations may be further below the altitude at which they formed than is the case for coastal cirques. If so, correcting CFAs for residual glacial isostatic adjustment would increase the inland gradient. In fact, glacial isostatic adjustment may help partly explain why the inland gradient in CFAs is steeper than for modern ELAs, since the former may have been affected by differential uplift since deglaciation, while the latter reflects the contemporary climate and is therefore independent of isostatic adjustment.

While there is regional variability in cirque lithology, there are no broad-scale trends to suggest that bedrock resistance increases with distance from the coast, certainly not in any way that explains overall trends in CFAs (unlike Delmas et al., 2014; Delmas et al., 2015). Finally, the dynamics of former cirque glaciers may have varied regionally, and there is evidence to indicate that coastal glaciers may have been more dynamic (with higher mass turnover). Additionally, the coastal, low-elevation glaciers would have only been covered by the ice sheet at maximum extent, and may have experienced greater time of active cirque glacier occupation than those in the interior that would have been shielded by cold-based ice (Olsen et al., 2001; Bakke et al., 2005; Batchelor et al., 2019). Any spatial differences in glacier dynamics are likely to result in differences in CFAs on the order of tens of metres (e.g. Dahl et al., 1997; Barr et al., 2017), not the hundreds of metres difference between the coast and peak mountains as observed.

5.2. Limitations of CFAs as palaeoclimate indicators

As outlined above, when glaciers are small, and largely confined to their cirques (i.e., during periods of cirque glaciation), CFAs roughly approximate cirque glacier ELAs, and could therefore be used (with some caveats) as a source of quantitative palaeoclimate information (precipitation and/or temperature). However, this palaeoclimatic information only becomes useful when it can be assigned to a particular time period. This requires geochronometric dating to establish when cirque-confined glaciers last occupied a landscape. This is possible through surface exposure dating (e.g., Barth et al., 2016; Barth et al., 2018), but it is expensive and impractical to apply to large populations, particularly when (as in the present study) thousands of cirques are considered. Without chronological information for many cirques, the palaeoclimatic inferences that can be drawn from populations are limited. Despite this caveat, trends in CFA may reflect general, longlasting or recurrent palaeoclimatic gradients – i.e. compound (palimpsest) gradients from the superimposition of several glacial phases. However, where CFAs track topography (as in the present study), isolating and quantifying the climatic component is difficult. Where CFA trends differ from modern ELA or climate trends, this might indicate changing climate (i.e., precipitation) patterns through time (e.g., Evans, 1999). However, in almost all cases, trends in CFA generally track modern climate/ELA (Peterson and Robinson, 1969; Hassinen, 1998; Anders et al., 2010; Barr and Spagnolo, 2015b; Barr et al., 2017; Wallick and Principato, 2020), and obtaining any useful palaeoclimatic information (beyond establishing that broad precipitation gradients have changed little through time – as observed in the present study) relies on interpreting differences between the two (e.g., Barr and Spagnolo, 2015b). However, in Scandinavia, even extracting palaeoclimatic information in this way is complicated by the potential role that the glacial history has played in regulating CFAs (Section 5.1.3.).

6. Conclusions

In this study, 3984 cirque floor altitudes (CFAs) and 513 modern cirque glacier ELAs were analysed across the Scandinavian Peninsula. We investigated trends in these data to establish controls on past and present glaciers in the region, and to establish what palaeoclimatic information can be obtained from CFAs. The main study findings are:

1. Latitudinal and aspect-related trends in CFA and modern glacier ELAs suggest that air temperatures and local shading played, and continue to play, a role in regulating sites of mountain glaciation across the Scandinavian Peninsula.
2. The dominant trend in CFAs and modern glacier ELAs across the region is an increase inland i.e., increasing with distance from the coast. These trends likely reflect the combined influence of climatic gradients (controlling past and present ELAs), and topographic gradients (restricting where glaciers and cirques can form). In the case of CFAs, unravelling controls on the increase inland is further complicated by spatial differences in glacial history (in particular, ice sheet growth in the interior during glacial periods, preventing the formation of low altitude cirques).
3. Results from the present study, supported by other studies, suggest that individual CFAs can yield useful (quantitative), but limited, palaeoclimate information. However, given the potential role of climate, topography, and glacial history (and the difficulties with disentangling these controls), palaeoclimatic interpretations derived from cirque populations and/or CFA trends should be treated with caution.

Declaration of Competing Interest

The authors whose names are listed immediately below certify that they have NO affiliations with or involvement in any organization or entity with any financial interest (such as honoraria; educational grants; participation in speakers' bureaus; membership, employment, consultancies, stock ownership, or other equity interest; and expert testimony or patent-licensing arrangements), or non-financial interest (such as personal or professional relationships, affiliations, knowledge or beliefs) in the subject matter or materials discussed in this manuscript.

Acknowledgements

The Scottish Alliance for Geoscience, Environment and Society (SAGES) and the University of Aberdeen are thanked for funding the PhD studentship awarded to Rachel P. Oien. I am grateful for the data provided by various scientists at the NVE and NGU in order to make this project possible. We thank Ian Evans, and an anonymous reviewer for their extremely helpful corrections, comments, and suggestions.

References

Agrell, H., 1977. A Glacial Cirque Form in Central Sweden? Geogr. Annaler, Series A: Phys. Geogr. 59 (3/4), 215–219.
Anders, A.M., Mitchell, S.G., Tomkin, J.H., 2010. Cirques, peaks, and precipitation patterns in the Swiss Alps: Connections among climate, glacial erosion, and topography. Geology 38 (3), 239–242. https://doi.org/10.1130/G30691.1.
Argus, D.F., Peltier, W.R., 2010. Constraining models of postglacial rebound using space geodesy: a detailed assessment of model ICE-5G (VM2) and its relatives. Geophys. J. Int. 697–723. https://doi.org/10.1111/j.1365-246X.2010.04562.x.
Bacon, S.N., Chinn, T.J., Van Dissen, R.J., Tillinghast, S.F., Goldstein, H.L., Burke, R.M., 2010. New Zealand Journal of Geology and Geophysics Paleo-equilibrium line altitude estimates from late Quaternary glacial features in the Inland Kaikoura Range, South Island, New Zealand. N. Z. J. Geol. Geophys. 44 (1), 55–67. https://doi.org/10.1080/00288306.2001.9514922.
Bakke, J., Dahl, S.O., Paasche, Ø., Løvlie, R., Nesje, A., 2005. Glacier fluctuations, equilibrium-line altitudes and palaeoclimate in Lyngen, northern Norway, during the Lateglacial and Holocene. The Holocene 15 (4), 518–540. https://doi.org/10.1191/0959683605hl815rp.
Bakke, J., Lie, Ø., Dahl, S.O., Nesje, A., Bjune, A.E., 2008. Strength and spatial patterns of the Holocene wintertime westerlies in the NE Atlantic region. Glob. Planet. Chang. 60 (1–2), 28–41. https://doi.org/10.1016/j.gloplacha.2006.07.030.
Barr, I.D., Spagnolo, M., 2013. Palaeoglacial and palaeoclimatic conditions in the NW Pacific, as revealed by a morphometric analysis of cirques upon the Kamchatka Peninsula. Geomorphology 192, 15–29. https://doi.org/10.1016/j.geomorph.2013.03.011.
Barr, I.D., Spagnolo, M., 2015a. Understanding controls on cirque floor altitudes: Insights from Kamchatka. Geomorphology 248, 1–13. https://doi.org/10.1016/j.geomorph.2015.07.004.
Barr, I.D., Spagnolo, M., 2015b. Glacial cirques as palaeoenvironmental indicators: their potential and limitations. Earth Sci. Rev. 151 (0), 48–78. https://doi.org/10.1016/j.earscirev.2015.10.004.
Barr, I.D., Ely, J.C., Spagnolo, M., Clark, C.D., Evans, I.S., Pellicer, X.M., Rea, B.R., 2017. Climate patterns during former periods of mountain glaciation in Britain and Ireland: Inferences from the cirque record. Palaeogeogr. Palaeoclimatol. Palaeoecol. 485, 466–475. https://doi.org/10.1016/j.palaeo.2017.07.001.
Barth, A.M., Clark, P.U., Clark, J., McCabe, A.M., Caffee, M., 2016. Last Glacial Maximum cirque glaciation in Ireland and implications for reconstructions of the Irish Ice Sheet. Quat. Sci. Rev. 141, 85–93. https://doi.org/10.1016/j.quascirev.2016.04.006.
Barth, A.M., Clark, P.U., Clark, J., Roe, G.H., Marcott, S.A., Marshall McCabe, A., Caffee, M.W., He, F., Cuzzone, J.K., Dunlop, P., 2018. Persistent millennial-scale glacier fluctuations in Ireland between 24 ka and 10 ka. Geology 46 (2), 151–154. https://doi.org/10.1130/G39796.1.
Batchelor, C.L., Margold, M., Krapp, M., Murton, D.K., Dalton, A.S., Gibbard, P.L., Stokes, C.R., Murton, J.B., Manica, A., 2019. The configuration of Northern Hemisphere ice sheets through the Quaternary. Nat. Commun. https://doi.org/10.1038/s41467-019-11601-2.
Benn, Douglas I., Lehmkuhl, F., 2000. Mass balance and equilibrium-line altitudes of glaciers in high-mountain environments. Quat. Int. 65 (66), 15–29.
Bjune, A.E., Bakke, J., Nesje, A., Birks, H.J.B., 2005. Holocene mean July temperature and winter precipitation in western Norway inferred from palynological and glaciological lake-sediment proxies. The Holocene 15 (2), 177–189.
Caseldine, C., Stotter, J., 1993. "Little Ice Age" glaciation of Trollaskagi peninsula, northern Iceland: climatic implications for reconstructed equilibrium line altitudes (ELAs). The Holocene 3 (4), 357–366. https://doi.org/10.1177/095968369300300408.
Coleman, C.G., Carr, S.J., Parker, A.G., 2009. Modelling topoclimatic controls on palaeoglaciers: implications for inferring palaeoclimate from geomorphic evidence. Quat. Sci. Rev. 28 (3–4), 249–259. https://doi.org/10.1016/j.quascirev.2008.10.016.
Dahl, S.O., Nesje, A., 1992. Paleoclimatic implications based on equilibrium-line altitude depressions of reconstructed Younger Dryas and Holocene cirque glaciers in inner Nordfjord, western Norway. In. Palaeogeogr. Palaeoclimatol. Palaeoecol. 94.
Dahl, S.O., Nesje, A., Øvstedal, J., 1997. Cirque glaciers as morphological evidence for a thin Younger Dry as ice sheet in east-central southern Norway. Boreas 26 (3), 161–180. https://doi.org/10.1111/j.1502-3885.1997.tb00850.x.
Delmas, M., Gunnell, Y., Calvet, M., 2014. Environmental controls on alpine cirque size. Geomorphology 206, 318–329. https://doi.org/10.1016/j.geomorph.2013.09.037.
Delmas, M., Gunnell, Y., Calvet, M., 2015. A critical appraisal of allometric growth among alpine cirques based on multivariate statistics and spatial analysis. Geomorphology 228, 637–652. https://doi.org/10.1016/j.geomorph.2014.10.021.
Etzelmüller, B., Romstad, B., Fjellanger, J., 2007. Automatic regional classification of topography in Norway. In. Nor. J. Geol. 87.
Evans, I.S., 1977. World-Wide Variations in the direction and Concentration of Cirque and Glacier Aspects. Geogr. Annaler, Series A: Phys. Geogr. 59 (3/4), 151–175 doi: https://www.jstor.org/stable/520797.
Evans, I.S., 1999. Was the cirque glaciation of Wales time-transgressive, or not? Ann. Glaciol. 28, 33–39. https://doi.org/10.3189/172756499781821652.
Evans, I.S., 2006a. Local aspect asymmetry of mountain glaciation: a global survey of consistency of favoured directions for glacier numbers and altitudes. Geomorphology 73, 166–184.
Evans, I.S., 2006b. Glacier distribution in the Alps : Statistical Modelling of Altitude and Aspect. Geogr. Annaler, Series A: Phys. Geogr. 88 A (2), 115–133. https://doi.org/10.1111/j.0435-3676.2006.00289.x.

Evans, I.S., 2011. Glacier distribution and direction in Svalbard, Axel Heiberg Island and throughout the Arctic: general northward tendencies. Polish Polar Res. 32, 199–238.
Evans, I.S., Cox, N., 1974. Geomorphometry and the operational definition of cirques. Area 6 (2), 150–153.
Forsström, P.-L., 2005. Through a glacial cycle: simulation of the Eurasian ice sheet dynamics during the last glaciation. Ann. Acad. Sci. Fennicae Geol. Geogr. 168, 1–94.
Fredin, O., 2002. Glacial inception and Quaternary mountain glaciations in Fennoscandia. Quat. Int. 95–96, 99–112. https://doi.org/10.1016/S1040-6182(02)00031-9.
Hassinen, S., 1998. A morpho-statistical study of cirques and cirque glaciers in the Senja-Kilpisjärvi area, northern Scandinavia. Nor. Geogr. Tidsskr. Norw. J. Geogr. 52 (1), 27–36. https://doi.org/10.1080/00291959808552381.
Hughes, A.L.C., Gyllencreutz, R., Lohne, Ø.S., Mangerud, J., Svendsen, J.I., 2016. The last Eurasian ice sheets – a chronological database and time-slice reconstruction, DATED-1. Boreas 45 (1), 1–45. https://doi.org/10.1111/bor.12142.
Holtedahl, O., 1920. The Scandinavian Mountain Problem. Quarter. J. Geol. Soc. 76, 387–403. https://doi.org/10.1144/GSL.JGS.1920.076.01-04.11.
Hughes, P.D., 2010. Little Ice Age glaciers in the Balkans: Low altitude glaciation enabled by cooler temperatures and local topoclimatic controls. Earth Surf. Process. Landf. 35 (2), 229–241. https://doi.org/10.1002/esp.1916.
Ipsen, H.A., Principato, S.M., Grube, R.E., Lee, J.F., 2018. Spatial analysis of cirques from three regions of Iceland: implications for cirque formation and palaeoclimate. Boreas 47, 565–576.
Kern, Z., László, P., 2010. Size specific steady-state accumulation-area ratio: an improvement for equilibrium-line estimation of small palaeoglaciers. Quat. Sci. Rev. 29 (19–20), 2781–2787. https://doi.org/10.1016/j.quascirev.2010.06.033.
Kleman, J., Stroeven, A.P., Lundqvist, J., 2008. Patterns of Quaternary ice sheet erosion and deposition in Fennoscandia and a theoretical framework for explanation. Geomorphology 97 (1–2), 73–90. https://doi.org/10.1016/j.geomorph.2007.02.049.
Křížek, M., Mida, P., 2013. The influence of aspect and altitude on the size, shape and spatial distribution of glacial cirques in the High Tatras (Slovakia, Poland). Geomorphology 198, 57–68. https://doi.org/10.1016/j.geomorph.2013.05.012.
Lambeck, K., Smither, C., Ekman, M., 1998a. Tests of glacial rebound models for Fennoscandinavia based on instrumented sea- and lake-level records. Geophys. J. Int. 135 (2), 375–387. https://doi.org/10.1046/j.1365-246X.1998.00643.x.
Lambeck, K., Smither, C., Johnston, P., 1998b. Sea-level change, glacial rebound and mantle viscosity for northern Europe. Geophys. J. Int. 134 (1), 102–144. https://doi.org/10.1046/j.1365-246X.1998.00541.x.
Lidmar-Bergström, K., Ollier, C.D., Sulebak, J.R., 2000. Landforms and uplift history of southern Norway. Glob. Planet. Chang. 24 (3–4), 211–231. https://doi.org/10.1016/S0921-8181(00)00009-6.
Mangerud, J., 2008. The early and middle Weichselian in Norway: a review. Boreas 10 (4), 381–393. https://doi.org/10.1111/j.1502-3885.1981.tb00500.x.
Mangerud, J., Gyllencreutz, R., Lohne, Ø., Svendsen, J.I., 2011. Glacial history of Norway. Dev. Qua. Sci. Vol 15, 279–298. ISSN: 1571-0866. https://doi.org/10.1016/B978-0-444-53447-7.00022-2.
Meierding, T.C., 1982. Late Pleistocene glacial equilibrium-line altitudes in the Colorado Front Range: a comparison of methods. Quat. Res. 18 (3), 289–310. https://doi.org/10.1016/0033-5894(82)90076-X.
Mitchell, S.G., Humphries, E.E., 2014. Glacial cirques and the relationship between equilibrium line altitudes and mountain range height. Geology 43 (1). https://doi.org/10.1130/G36180.1.
Morris, S.E., 1981. Topoclimatic Factors and the Development of Rock Glacier Facies. Arct. Alp. Res. 13 (3), 329–338. https://doi.org/10.1080/00040851.1981.12004253.
Nesje, A., 1992. Topographical effects on the equilibrium line altitude on glaciers. GeoJournal 27, 383–391.
Nesje, A., 2009. Latest Pleistocene and Holocene alpine glacier fluctuations in Scandinavia. Quat. Sci. Rev. 28 (21–22), 2119–2136. https://doi.org/10.1016/j.quascirev.2008.12.016.
Nesje, A., Bakke, J., Dahl, S.O., Lie, Ø., Matthews, J.A., 2008. Norwegian mountain glaciers in the past, present and future. Glob. Planet. Chang. 60 (1–2), 10–27. https://doi.org/10.1016/j.gloplacha.2006.08.004.
Nielsen, S.B., Gallagher, K., Leighton, C., Balling, N., Svenningsen, L., Jacobsen, B.H., Thomsen, E., Nielsen, O.B., Heilmann-Clausen, C., Egholm, D.L., Summerfield, M.A., Clausen, O.R., Piotrowski, J.A., Thorsen, M.R., Huuse, M., Abrahamsen, N., King, C., Lykke-Andersen, H., 2009. The evolution of western Scandinavian topography: a review of Neogene uplift versus the ICE (isostasy-climate-erosion) hypothesis. J. Geodyn. 47 (2–3), 72–95. https://doi.org/10.1016/j.jog.2008.09.001.
Norwegian Mapping Authority, . The Terrain Model WMS Service Provides Information on the Terrestrial Terrain Model (DTM 10). https://www.kartverket.no/data/Laserskanning/.
Norwegian Meteorological Institute, 2021. Climate Norms. Retrieved April 23, 2021, from Norwegian Centre for Climate Services website: https://klimaservicesenter.no/kss/vrdata/normaler.
NVE, 2017. Norwegian Water Resources and Energy Directorate (NVE). Climate Indicator Products. http://glacier.nve.no/viewer/CI/. downloaded b2017.12.01 N.
Ohmura, A., Boettcher, M., 2018. Climate on the equilibrium line altitudes of glaciers: Theoretical background behind Ahlmann's P/T diagram. J. Glaciol. 64 (245), 489–505. https://doi.org/10.1017/jog.2018.41.
Ohmura, At, Kasser, P., Funk, M., 1992. Climate at the equilibrium line of glaciers. J. Glaciol. 38 (130), 397–411. https://doi.org/10.3189/S0022143000002276.
Oien, R.P., Spagnolo, M., Rea, B.R., Barr, I.D., Bingham, R.G., 2020. Climatic controls on the equilibrium-line altitudes of Scandinavian cirque glaciers. Geomorphology 352. https://doi.org/10.1016/j.geomorph.2019.106986.
Olsen, L., Sveian, H., Bergstrom, B., 2001. Rapid adjustments of the western part of the Scandinavian ice sheet during the Mid- and Late Weichselian a new model. Nor. Geogr. Tidsskr. Nor. J. Geogr. 81 (93–118).
Olsen, L., Sveian, H., Bergstrøm, B., Ottesen, D., Rise, L., 2013a. Quaternary glaciations and their variations in Norway and on the Norwegian continental shelf. Quat. Geol. Norway, Geol. Survey Norway Spec. Publ. 13, 27–78.
Olsen, L., Sveian, H., Ottesen, D., Rise, L., 2013b. Quaternary glacial, interglacial and interstadial deposits of Norway and adjacent onshore and offshore areas. Quat. Geol. Norway, Geol. Survey Norway Spec. Publ. 13, 79–144.
Olyphant, G.A., 1977. Topoclimate and the Depth of Cirque Erosion. Geogr. Annaler, Series A: Phys. Geogr. 59 (3), 209–213. Retrieved from. https://www.jstor.org/stable/520800.
Pawlewicz, M.J., Steinshouer, D.W., Gautier, D.L., 2002. Map showing geology, oil and gas fields, and geologic provinces of Europe including Turkey: U.S. Geological Survey Open-File Report 97–470-I, 14 p. https://doi.org/10.3133/ofr97470I.
Pearce, D.M., Ely, J.C., Barr, I.D., Boston, C.M., 2017. Section 3.4.9: Glacier Reconstruction. In Geomorphological Techniques (Online Edition) (Vol. 9). Br. Soc. Geomorph. 9, 1–16.
Pedersen, V.K., Knutsen, Å.R., Pallisgaard-Olesen, G., Andersen, J.L., Moucha, R., Huismans, R.S., 2021. Widespread glacial erosion on the Scandinavian passive margin. Geology 49 (8), 1004–1008. https://doi.org/10.1130/g48836.1.
Peterson, J.A., Robinson, G., 1969. Trend surface mapping of cirque floor levels. Nature 222, 75–76. https://doi.org/10.1038/222075a0.
Principato, S.M., Lee, J.F., 2014. GIS analysis of cirques on Vestfirdir, northwest Iceland: Implications for palaeoclimate. Boreas 43 (4), 807–817. https://doi.org/10.1111/bor.12075.
Rea, B.R., Pellitero, R., Spagnolo, M., Hughes, P., Ivy-Ochs, S., Renssen, H., Ribolini, A., Bakke, J., Lukas, S., Braithwaite, R.J., 2020. Atmospheric circulation over Europe during the Younger Dryas. Science. Advances 6 (50), eaba4844. https://doi.org/10.1126/sciadv.aba4844.
Renssen, H., Isarin, R.F.B., Jacob, D., Podzun, R., Vandenberghe, J., 2001. Simulation of the Younger Dryas climate in Europe using a regional climate model nested in an AGCM: preliminary results. Glob. Planet. Chang. 30, 41–57.
Rosentau, A., Harff, J., Oja, T., Meyer, M., 2012. Postglacial rebound and relative sea level changes in the Baltic Sea since the Litorina transgression. Baltica 25 (2), 113–120. https://doi.org/10.5200/baltica.2012.25.11.
Rudberg, S., 1994. Glacial cirques in Scandinavia. Nor. Geogr. Tidsskr. Nor. J. Geogr. 48 (4), 179–197. https://doi.org/10.1080/00291959408552343.
Seppä, H., Birks, H.J.B., 2001. July mean temperature and annual precipitation trends during the Holocene in the Fennoscandian tree-line area: pollen-based climate reconstructions. The Holocene 11 (5), 527–539.
Spagnolo, M., Pellitero, R., Barr, I.D., Ely, J.C., Pellicer, X.M., Rea, B.R., 2017. ACME, a GIS tool for Automated Cirque Metric Extraction. Geomorphology 278, 280–286. https://doi.org/10.1016/j.geomorph.2016.11.018.
Steer, P., Huismans, R.S., Valla, P.G., Gac, S., Herman, F., 2012. Bimodal plio-quaternary glacial erosion of fjords and low-relief surfaces in Scandinavia. Nat. Geosci. 5 (9), 635–639. https://doi.org/10.1038/ngeo1549.
Steffen, H., Kaufmann, G., 2005. Glacial isostatic adjustment of Scandinavia and northwestern Europe and the radial viscosity structure of the Earth's mantle. Geophys. J. Int. 163 (2), 801–812. https://doi.org/10.1111/j.1365-246X.2005.02740.x.
Stephens, M.B., 1988. The Scandinavian Caledonides: a complexity of collisions. Geol. Today 4 (1), 20–26. https://doi.org/10.1111/j.1365-2451.1988.tb00537.x.
Stroeven, A.P., Hättestrand, C., Kleman, J., Heyman, J., Fabel, D., Fredin, O., Goodfellow, B.W., Harbor, J.M., Jansen, J.D., Olsen, L., Caffee, M.W., Fink, D., Lundqvist, J., Rosqvist, G.C., Strömberg, B., Jansson, K., 2016. Deglaciation of fennoscandia. Quat. Sci. Rev. 147, 91–121. https://doi.org/10.1016/j.quascirev.2015.09.016.
Sutherland, D.G., 1984. Modern glacier characteristics as a basis for inferring former climates with particular reference to the Loch Lomond Stadial. Quat. Sci. Rev. 3 (4), 291–309. https://doi.org/10.1016/0277-3791(84)90010-6.
Torsnes, I., Rye, N., Nesje, A., 1993. Arctic and Alpine Research Modern and Little Ice Age Equilibrium-line Altitudes on Outlet Valley Glaciers from Jostedalsbreen, Western Norway: An Evaluation of Different Approaches to their Calculation. Arct. Alp. Res. 25 (2), 106–116. https://doi.org/10.1080/00040851.1993.12002990.
Tveito, O.E., Førland, E., Heino, R., Hansen-Bauer, I., Alexandersson, H., Dahlström, B., Drebs, A., Kern-Hansen, C., Jónsson, T., Laursen, E.V., Westman, Y., 2000. DNMI - Nordic temperature maps. In: DNMI - Report: Vol. 09/00 KLIM. Norwegian Meterological Institute.
Vilborg, L., 1977. The Cirque Forms of Swedish Lapland Author. Geogr. Annaler, Series A: Phys. Geogr. 59 (3), 89–150 doi. https://www.jstor.org/stable/520796.
Vilborg, L., 1984. The Cirque Forms of Central Sweden. Geogr. Annaler, Series A: Phys. Geogr. 66 (1), 41–77 doi: https://www.jstor.org/stable/520939.
Wallick, K.N., Principato, S.M., 2020. Quantitative analyses of cirques on the Faroe Islands: evidence for time transgressive glacier occupation. Boreas 49 (4), 828–840. https://doi.org/10.1111/bor.12458.
Winkler, S., Elvehy, H., Nesje, A., 2009. Glacier fluctuations of Jostedalsbreen, western Norway, during the past 20 years: The sensitive response of maritime mountain glaciers. The Holocene 19 (3), 395–414. https://doi.org/10.1177/0959683608101390.
Winsvold, S.H., Andreassen, L.M., Kienholz, C., 2014. Glacier area and length changes in Norway from repeat inventories. Cryosphere 8, 1885–1903. https://doi.org/10.5194/tc-8-1885-2014.